Published in final edited form as:
Cancer Res. 2014 April 15; 74(8): 2152–2159. doi:10.1158/0008-5472.CAN-13-0813.

Detection of Brain Tumor Cells in the Peripheral Blood by a Telomerase Promoter-Based Assay

Kelly M. MacArthur[1], **Gary D. Kao**[1], **Sanjay Chandrasekaran**[1], **Michelle Alonso-Basanta**[1], **Christina Chapman**[1], **Robert A. Lustig**[1], **E. Paul Wileyto**[2], **Stephen M. Hahn**[1], and **Jay F. Dorsey**[1]

[1]Departments of Radiation Oncology, Perelman School of Medicine, University of Pennsylvania, Philadelphia, Pennsylvania

[2]Departments of Biostatistics and Epidemiology, Perelman School of Medicine, University of Pennsylvania, Philadelphia, Pennsylvania

Abstract

Blood tests to detect circulating tumor cells (CTC) offer great potential to monitor disease status, gauge prognosis, and guide treatment decisions for patients with cancer. For patients with brain tumors, such as aggressive glioblastoma multiforme, CTC assays are needed that do not rely on expression of cancer cell surface biomarkers like epithelial cell adhesion molecules that brain tumors tend to lack. Here, we describe a strategy to detect CTC based on telomerase activity, which is elevated in nearly all tumor cells but not normal cells. This strategy uses an adenoviral detection system that is shown to successfully detect CTC in patients with brain tumors. Clinical data suggest that this assay might assist interpretation of treatment response in patients receiving radiotherapy, for example, to differentiate pseudoprogression from true tumor progression. These results support further development of this assay as a generalized method to detect CTC in patients with cancer.

Corresponding Author: Jay F. Dorsey, Smilow Center for Translational Research, Perelman School of Medicine, University of Pennsylvania, Building 421 Room 8-135, 3400 Civic Center Boulevard, Philadelphia, PA 19104-5156. Phone: 215-898-1080; Fax: 215-898-0090; JayD@uphs.upenn.edu.
K.M. MacArthur and G.D. Kao are the first co-authors of this article.

Note: Supplementary data for this article are available at Cancer Research Online (http://cancerres.aacrjournals.org/).

Disclosure of Potential Conflicts of Interest
The coauthors are employees of the University of Pennsylvania, which has a patent pending on components of the technology described in this manuscript. J.F. Dorsey, G.D. Kao, and S.M. Hahn are cofounders of Liquid Biotech LLC (Penn CTT/ UpSTART). No potential conflicts of interest were disclosed by the other authors.

Authors' Contributions
Conception and design: G.D. Kao, C. Chapman, R.A. Lustig, S.M. Hahn, and J.F. Dorsey
Development of methodology: K.M. MacArthur, G.D. Kao, C. Chapman, and J.F. Dorsey
Acquisition of data (provided animals, acquired and managed patients, provided facilities, etc.): K.M. MacArthur, G.D. Kao, M. Alonso-Basanta, C. Chapman, R.A. Lustig, S.M. Hahn, and J.F. Dorsey
Analysis and interpretation of data (e.g., statistical analysis, biostatistics, computational analysis): K.M. MacArthur,G.D. Kao, C. Chapman, E.P.Wileyto, S.M. Hahn, and J.F. Dorsey
Writing, review, and/or revision of the manuscript: K.M. MacArthur, G.D. Kao, S. Chandrasekaran, M. Alonso-Basanta, C. Chapman, R.A. Lustig, E.P. Wileyto, S.M. Hahn, and J.F. Dorsey
Administrative, technical, or material support (i.e., reporting or organizing data, constructing databases): S. Chandrasekaran, C. Chapman, and J.F. Dorsey
Study supervision: G.D. Kao, M. Alonso-Basanta, R.A. Lustig, and J.F. Dorsey

Introduction

High-grade brain tumors are often markedly aggressive and associated with a poor prognosis. For example, despite combination therapy that typically consists of surgical resection, radiotherapy (1), and systemic chemotherapy (both concurrent and adjuvant; ref. 2), glioblastoma multiforme (grade 4 glioma) remains the most fatal primary malignant central nervous system neoplasm in adults, with a median overall survival of 14.6 months. The management of patients with brain tumors often includes additional challenges such as accurately differentiating tumor progression from pseudo-progression (3), the latter of which consists of treatment-related changes to the normal vasculature and often results in increased signal intensity that is difficult to distinguish from enhancing tumor tissue on MRI studies.

Given the poor prognoses associated with high-grade brain tumors, such as gliomas, and the difficulties monitoring tumor response or progression, there is clearly a need for innovative approaches to improve tumor assessment. Circulating biomarkers are a promising, noninvasive means to evaluate the status of the primary brain tumor, and may potentially help in guiding patient treatment and management in the future. In this regard, we describe here the novel application of a telome-rase-based assay for detecting circulating brain tumor cells, effective in cell culture and animal studies, and in a pilot cohort of patients with high-grade glioma.

Materials and Methods

Cell culture, Western blot analysis, and immunofluorescence

Human glioma cell lines U251 [World Health Organization (WHO) grade IV], U87 (WHO grade IV), and U373 (WHO grade III; along with control cell lines SKBR3 (human breast cancer) and PC3 (human prostate cells) were purchased from the American Type Culture Collection and were maintained in Dulbecco's Modified Eagle Medium (DMEM; Invitrogen) supplemented with 10% FBS (Invitrogen) and 1.0% penicillin–streptomycin at 37°C in an atmosphere of 5%CO_2. For immunoblotting, 3×10^5 cells were seeded into each well of a 6-well culture plate and left undisturbed for 24 hours, before lysis with 100 μL of 2× Laemmli sample buffer. The cell lysates were subsequently boiled for 5 minutes and centrifuged to remove cell debris. An equal volume of each cell lysate sample (15 μL) was loaded into the individual wells of a NuPAGE Novex 4% to 12% Bis–Tris gel (Invitrogen) and resolved by electrophoresis in 1× NuPAGE MOPS SDS Running Buffer (Invitrogen) for 1:20 hours at 125 V. Of note, 20 μL of 2.4 μg/μL of normal brain extract (Santa Cruz Biotechnology, Inc.) served as a negative control. The See-BluePlus2 prestained protein standards (Invitrogen) was included (12 μL/well) for protein size determination. Electrophoretic transfer onto polyvinylidene difluoride (PVDF) membrane was performed with 1× NuPAGE Transfer Buffer (Invitrogen) at 30 V for 1 hour. Membranes were then blocked with 5% (*w/v*) dried nonfat milk in PBST buffer (1× PBS containing 0.06% Tween 20) for 1 hour at room temperature and then incubated with primary antibodies. Immuno-blotting for Nestin (1:1,000, mouse, clone 10C2; Abcam Inc.), Ran (1:20,000, mouse monoclonal; BD Transduction Laboratories), EGF receptor (EGFR; Cell Signaling Technology), and β-actin (1:1,000, clone AC-15; Sigma-Aldrich) was performed overnight

at 4°C. Alternatively, immunoblotting for epithelial cell adhesion molecule (EpCAM; 1:500, mouse, clone #158210; R&D Systems) and human telomerase reverse transcriptase (hTERT; 1:500, rabbit, clone Y182; Millipore) was performed for 2 hours at room temperature. Following incubations with primary antibodies, membranes were washed in PBST buffer and incubated with horseradish peroxidase–conjugated secondary antibodies (Amersham, GE Healthcare) for 1 hour at room temperature. All antibodies were diluted in PBST-5% milk buffer. Immunoreactive bands were visualized via enhanced chemiluminescence by incubating membranes with the ECL Western Blotting Detection Reagents in accordance with the manufacturer's recommendations (Amersham, GE Healthcare). Films were exposed to the membranes for the appropriate durations and subsequently scanned with a personal scanner (Epson Perfection 4490 photo). The specificity of the anti-EGFR antibody was tested (via Western blotting or immunofluorescence) on cell lines known to express or to be deficient for EGFR (Supplementary Fig. S2). Immunofluorescence was performed on formalin- or formaldehyde-fixed cells (1% formalin, 10-minute duration at room temperature), with incubation with primary antibodies for 1 hour, followed by incubation for 30 minutes with fluorochrome-conjugated secondary antibodies (Molecular Probes).

Orthotopic brain tumor xenografts in mice

U251 cells constitutively expressing GFP and luciferase were orthotopically implanted in a nude, athymic mouse as per previously published protocol (4, 5). Brain tumor growth was confirmed and tracked via serial bioluminescence imaging, before removal, sectioning, and formalin fixation. The brain tumor sections were subsequently stained for hematoxylin and eosin (H&E) or for immunofluorescence with the following antibodies: Nestin (Abcam), EpCAM (R&D Systems), glial fibrillary acidic protein (GFAP; Invitrogen), and 4′,6-diamidino-2-phenylindole (DAPI; Vector Laboratories).

Adenoviral probe for tumor cell detection

The tumor cell detection assay uses a telomerase-responsive adenoviral probe that consist of the expression cassette for GFP (inserted within the deleted E3 region), as well as the hTERT promoter driving expression of E1A and E1B for viral replication and amplification of the GFP signal (TelomeScan; Oncolys; ref. 6). The efficacy of the probe in glioma cell lines was first characterized via time-course experiments and immunofluorescence staining. For these experiments, cells were seeded onto 8-well poly-D-lysine–coated chamber slides (typically 5×10^3 cells/well) before viral infection. The probe ($2 \times 10E8$ viral particles) was introduced into each well and time-lapse phase contrast and fluorescent microscopy images were taken every 6 hours for the duration of each experiment.

Analysis of patient samples

After receiving written informed consent, peripheral blood collections were obtained from patients or healthy control volunteers under Institutional Review Board–approved protocols. All patients in the study were free of significant comorbid medical conditions or prior cancer, deemed operable, and underwent biopsy, subtotal, or gross total surgical resection, followed by radiotherapy. Peripheral blood was also obtained from healthy, cancer-free adult volunteers, and processed alongside patient samples, to serve as controls. To determine a circulating tumor cell (CTC) threshold in patients, we conducted an analysis of 30 blood

samples collected from healthy volunteers. This analysis determined a threshold of 1.3 GFP-positive cells/mL of blood from healthy controls as the "baseline" for determining whether a patient was considered to have detectable CTCs. To minimize the risk of inadvertent collection of epithelial stem cells, the initial tube of collected blood was discarded. For each patient, approximately 10 mL of peripheral blood was collected into green-top vacutainer tubes containing the anticoagulant heparin. The collected blood was then centrifuged in OncoQuick tubes as per a protocol adapted from the manufacturer's recommendations to remove red blood cells (RBC) and other non-CTC constituents of the blood. The resulting CTC-enriched layer was removed for further washing. The purified CTCs were then placed into media-contained chamber slides, and incubated in the presence of the adenoviral probe for 24 hours at 37°C and then fixed. The CTC-containing chamber wells were then imaged via a computer-driven semiautomated fluorescence microscope, with subsequent analysis performed via Image-Pro Plus. Analysis included sorting and filtering based on reproducible parameters such as fluorescent intensity (five SDs above background), cell area, cell diameter (between 15 and 70 μm), and absence of clumping or debris. The resultant data can therefore identify tumor cells with specificity, which are identified as brightly fluorescent due to the probe while also excluding debris and clumped cells (Supplementary Fig. S2).

Statistical methods

Data were summarized as counts/mL. We analyzed data using an ANOVA model estimated in a Generalized Linear Models regression framework, using a negative binomial link for the cell count outcome. We accounted for repeated measures from the same subject using the cluster-correlated robust covariance estimate to adjust standard errors. Models treated time point/control status as a categorical variable, and treated the before treatment condition as the reference group. A logistic regression-based classifier (applied to all data) was used to discriminate between control (n = 30) and pretreatment (n = 11) levels. To define patients with CTC-detectable disease, we then used the classifier to determine a threshold of 1.3 cells/mL (demarcated as "T" in Fig. 4A and B).

Results and Discussion

Our initial experiments included those for establishing the specificity of the probe, and testing the usefulness of Nestin as a glioma cell marker for immunofluorescence and subsequent CTC analysis. Glioma cells do not express EpCAM (7, 8), commonly used for CTC detection. All glioma cell lines we tested (U251, U373, and U87) showed varying levels of Nestin expression, but virtually no EpCAM. In contrast, EpCAM but not Nestin was detected in breast (SKBR3) and prostate cancer (PC3) cell lines (Fig. 1A). Moreover, the absence of EpCAM expression in glioma was confirmed via immunofluorescence staining of U251 glioma cells in culture with PC3 prostate cancer cells used as positive control (Fig. 1B). The usefulness of Nestin as a glioma marker was also confirmed in an *in vivo* model of glioma. In this system, human glioma cells were implanted into nude mice to generate orthotopic brain tumors as previously described (4, 5). As shown in Fig. 1C, the resultant tumors continue to express Nestin and show absence of EpCAM *in vivo*. As an additional test of tumor demarcation, we stained the sections for GFAP, which also readily identified the tumor due to its glial origin. Finally, as our ultimate goal was to track tumor

cells based on elevated telomerase expression (9, 10), the brain tumor sections were stained for the presence of human telomerase (hTERT). As expected, hTERT showed specific *in vivo* tumor staining similar to that of Nestin (Fig. 1C).

The colocalization of Nestin and telomerase in our brain tumor model in contrast to the lack of either in normal brain was encouraging for utilization of elevated telomerase as a marker of glioma tumor cells. We have confirmed that all brain tumor cell lines (as well as cancer cell lines from other tumor histologies) tested show elevated levels of telomerase, while normal brain (either human or mouse) does not (Fig. 1D and data not shown). We next established the effect of the telomerase-detecting probe in glioma cells as a function of time and in the presence of control blood from healthy volunteers. Each of the glioma cell lines tested showed signal at 12 hours after exposure to probe, which was robust by 24 hours (Fig. 2A and B). The signal was durable and persisted to and beyond 48 hours after initial exposure (albeit the absolute numbers of cells were reduced because of cell death). Finally, we spiked control blood with human glioma cells grown in culture, which stably expressed the fluorescent tag mCherry to allow discernment from nontumor cells. The entire sample was then exposed to probe and imaged 24 hours later. As shown in the representative image in Fig. 2C, only the tumor cells expressed GFP after exposure to probe, resulting in complete concordance with mCherry fluorescence [resulting in only yellow cells when the respective images are merged (Merge), with no cells showing only GFP or mCherry alone]. In contrast, the nuclei of the white blood cells (WBC) in the sample also stain with the nuclear marker DAPI, but showed neither GFP nor mCherry fluorescence. Additional experiments with time-lapse microscopy confirmed the lack of GFP false-positive signal in processed control blood from healthy volunteers exposed to the telomerase-based CTC probe (Supplementary Fig. S1A and S1B). These experiments together therefore established the specificity of the probe for accurately demarcating glioma cells while leaving normal cells unaffected.

We subsequently demonstrated that Nestin also serves as a useful marker of glioma-derived tumor cells in peripheral blood samples taken from patients. The probe identified tumor cells with elevated telomerase activity (via GFP expression), which was coincident with Nestin expression (Fig. 3A). In contrast, the nuclei of surrounding WBCs stained for DAPI but showed neither GFP nor Nestin expression. Furthermore, as an additional verification that the GFP-positive cells that we were identifying in patients with glioma were in fact derived from the primary tumor, we conducted immunofluorescence staining for EGFR in the CTCs from patients with tumors that demonstrated amplification of the EGFR. Figure 3 shows the results of a representative patient (with additional images in Supplementary Fig. S3). This was a patient with a WHO grade IV primary tumor who underwent resection, and with the resultant tissue found to have EGFR gene amplification based on solid tumor next-generation sequencing panel (Illumina TruSeq Amplicon-Cancer Panel). The amplification was reported as a 10- to 12-fold increase in the sequencing reads corresponding to the amplicons covering EGFR in the submitted tumor sample. Immunohistochemical analysis of the tumor resection specimen also noted strong EGFR protein expression in the majority of tumor cells. This genetic underpinning identified in the primary tumor provided us with the opportunity to test the patient's peripheral blood sample for CTCs, which should also show

overexpression of EGFR. We found that the probe identified tumor cells via GFP expression, and we subsequently confirmed that it showed strong EGFR overexpression (results with CTCs from additional patients with EGFR-overexpressing tumors are shown in Supplementary Fig. S5). These results together indicated that the probe was successful in accurately identifying glioma-derived CTCs in the peripheral circulation of patients with high-grade (and EGFR-overexpressing) glioma. In addition, EpCAM was not detectable in the CTCs of this patient, as well other patients with gliomas that lack EGFR overexpression (Supplementary Fig. S6).

Having established the potential usefulness of the probe, we initiated a pilot study to study CTCs in cohort of glioma patients undergoing radiotherapy in the Department of Radiation Oncology, Perelman School of Medicine (Philadelphia, PA). Peripheral blood samples were obtained from patients with pathology-confirmed primary high-grade (WHO grade III or IV) glioma, either before initiation of (Pre-RT) or following completion of cranial radiotherapy (Post-RT, total dose of 3,000–6,000 cGy). Healthy volunteer blood samples served as negative controls and were processed alongside patient samples (Fig. 4A). We found that CTCs were detectable in 8 of 11 (72%) preradiotherapy patients, compared with 1 of 8 (8%) postradiotherapy patients (Fig. 4B). In the preradiotherapy patients, there was a wide range of CTCs, but the average value was 8.8 CTC/mL of blood.

For a small number of the patients, sequential CTC counts were available and were especially illuminating. One patient (the second patient in Table 1) had been previously treated with adjuvant chemoradiation for high-grade glioma but then represented with obstructive hydrocephalus with MRI showing a cystic mass in the left thalamus. A ventriculoperitoneal shunt was placed and salvage radiation was prescribed (3,000 cGy). The first CTC analysis performed before the start of the salvage radiation was found to be 5.0 CTC/mL. Although the patient appeared stable in the initial post–re-irradiationperiod and with standard MRI appearing unchanged, the CTC count was however found to have increased posttreatment to 15.4 CTC/mL. Subsequent advanced MRI scans then demonstrated increased relative cerebral blood volume (rCBV) in the tumor supporting the early finding of progressive disease, and the patient was later confirmed to have tumor recurrence (Fig. 4C, left).

A second patient with high-grade glioma (Table 1 and Fig. 4C, right) was found to have a preradiotherapy count of 12.5 CTC/mL. The patient completed and tolerated chemoradiation without complications. A posttreatment MRI showed persistence of T2 signal (initially interpreted as: "progressive disease vs. treatment changes"), while the posttreatment CTC level of 1.0 CTC/mL indicated treatment response. In subsequent posttreatment visits, the patient'sMRI scans demonstrated improvement and therefore, the imaging findings were ultimately attributed to "pseudoprogression," not progressive disease.

Standard monitoring for treatment response and disease progression in patients with high-grade glioma can present challenges. Serial MRI obtained before and following completion of therapy is typically involved, but changes resulting from either "pseudoprogression" or radionecrosis may mimic progressive disease. "Pseudoprogression," commonly associated with temozolomide therapy, entails new MRI enhancement within 3 months of completion

of radiotherapy, which gradually resolves and thus nonindicative of true tumor progression. A "pseudoprogression" incidence of 31.1% was recently reported within a cohort of 103 patients with high-grade gliomas (11). Pseudoprogression is therefore often mistaken for true tumor progression, potentially resulting in great anxiety for patients and family as well as interfering with the accuracy of MRI in up to half of patients during the first postradiotherapy MRI (12, 13). Radionecrosis, which typically occurs within 3 to 12 months postradiotherapy (14), can further hamper the accurate diagnosis of tumor progression. Taken together, further research and development of additional tools to monitor tumor status, such as a brain tumor CTC assay, would be a welcome complement to radiographic imaging.

Although detection of CTCs from primary brain tumors presents a unique challenge, a number of technologies have been described for CTC purification and detection of tumors in general. Among the earliest were gradient separation fluid-based methods (e.g., Ficoll Paque) to separate CTCs from RBCs and WBCs and other constituents based on buoyant density (15). Isolation by size of epithelial tumor cells (ISET) method uses an 8-μm pore diameter filter to separate epithelial CTCs from hematopoetic cells, assuming the former to be larger than the latter (16), but overlapping pores created in the filter-manufacturing process may result in nonuniform pores. Newer generation systems have been created to attempt to improve and optimize CTC sensitivity (17). Among the most prominent is the CellSearch system (Veridex, LLC; ref. 18) that is based on the detection of EpCAM. Mikolajczyk and colleagues attempted to use EpCAM and cytokeratin and other antibody mixtures to identify a greater range of CTCs (19), but these systems may not be effective for tumors that do not express such surface markers, including brain tumors. Furthermore, epithelial-to-mesenchymal transition (EMT) may occur in tumors of epithelial origin, in which surface cell markers are downregulated and mesenchymal markers are upregulated, which may negatively affect assay performance (20–22). Of note, tumors that have undergone EMT may represent a more aggressive phenotype, portending worse prognosis (20) and treatment resistance (23).

We used a telomerase-based assay to detect CTCs in our patients with brain tumor. Telomerase is a protein expressed in most cancer cells that enables cell renewal by maintaining telomeres found at the end of chromosomes (9). Kojima and colleagues engineered an adenovirus containing the gene for GFP that can selectively replicate in cells that express telomerase (6). Because well-differentiated WBCs typically do not express telomerase, the fluorescence detected after replication can help distinguish CTCs from noncancerous cells found in the blood. The major advantage of a telomerase-based system is that this method is epithelial cell marker-independent. Although a telomerase-based strategy to identify CTCs has been used in other malignancies (24–26), our report highlights for the first time this approach for the detection of brain tumor–derived CTCs, which to our knowledge has not been reported in the literature previously.

In conclusion, we propose telomerase-based systems may be useful for CTC detection in patients with brain tumors, offering high sensitivity (as greater than 90% of solid tumors, including glioma, express elevated levels of telomerase; ref. 9) and high specificity (as telomerase is not found to be expressed in well-differentiated and normal cells). We

recognize the limitations of this study, including the need for more serial measurements throughout the treatment and disease course for each patient, and the small sample size (which does not permit sub-factor analysis). Furthermore, future investigation is warranted into characterizing the potentially unique genetic signatures expressed within the brain tumor CTCs that would allow for genetic stratification of patients including information on genetic subtypes and characteristics such as IDH1/2, EGFR, and PIK3CA (27). These efforts are currently being pursued in our ongoing studies.

The encouraging pilot data we describe have also prompted us to begin a new protocol to enroll a larger cohort of patients who will be serially followed through their treatment course and follow-up period (up to 2 years). The results of such prospective studies will be needed to establish the ultimate clinical utility of this telomerase-based brain tumor CTC assay.

Supplementary Material

Refer to Web version on PubMed Central for supplementary material.

Acknowledgments

The authors thank Emigdio Reyes, Melody Ju, David Steinmetz, James J. Davis, Wensheng Yang, and Xiangsheng Xu for their technical assistance. The authors also thank the Department of Radiation Oncology Clinical Research Coordinators for their assistance with sample collections and they acknowledge Oncolys Biopharma (Tokyo, Japan) for providing the Telomescan reagent for use in the experiments.

Grant Support

This work was supported by the Department of Radiation Oncology (Penn Medicine), the NIH (RC1 CA145075), National Institute of Neurological Disorders and Stroke (K08NS076548-01), and a Burroughs Wellcome Career Award for Medical Scientists (1006792). K.M. MacArthur was supported on the Radiation Biology Training Grant C5T32CA009677 (Principal Investigator: Dr. Ann Kennedy).

References

1. Imperato JP, Paleologos NA, Vick NA. Effects of treatment on long-term survivors with malignant astrocytomas. Ann Neurol. 1990; 28:818–822. [PubMed: 2178330]
2. Stupp R, Mason WP, van den Bent MJ, Weller M, Fisher B, Taphoorn MJ, et al. Radiotherapy plus concomitant and adjuvant temozolomide for glioblastoma. N Engl J Med. 2005; 352:987–996. [PubMed: 15758009]
3. Mehta AI, Kanaly CW, Friedman AH, Bigner DD, Sampson JH. Monitoring radiographic brain tumor progression. Toxins. 2011; 3:191–200. [PubMed: 22069705]
4. Baumann BC, Kao GD, Mahmud A, Harada T, Swift J, Chapman C, et al. Enhancing the efficacy of drug-loaded nanocarriers against brain tumors by targeted radiation therapy. Oncotarget. 2013; 4:64–79. [PubMed: 23296073]
5. Baumann BC, Dorsey JF, Benci JL, Joh DY, Kao GD. Stereotactic intracranial implantation and *in vivo* bioluminescent imaging of tumor xenografts in a mouse model system of glioblastoma multiforme. J Vis Exp. 2012; pii:4089. [PubMed: 23051742]
6. Kojima T, Hashimoto Y, Watanabe Y, Kagawa S, Uno F, Kuroda S, et al. A simple biological imaging system for detecting viable human circulating tumor cells. J Clin Invest. 2009; 119:3172–3181. [PubMed: 19729837]
7. Momburg F, Moldenhauer G, Hammerling GJ, Moller P. Immunohistochemical study of the expression of a Mr 34,000 human epithelium-specific surface glycoprotein in normal and malignant tissues. Cancer Res. 1987; 47:2883–2891. [PubMed: 3552208]

8. Moldenhauer G, Momburg F, Moller P, Schwartz R, Hammerling GJ. Epithelium-specific surface glycoprotein of Mr 34,000 is a widely distributed human carcinoma marker. Br J Cancer. 1987; 56:714–721. [PubMed: 2449234]
9. Kyo S, Inoue M. Complex regulatory mechanisms of telomerase activity in normal and cancer cells: how can we apply them for cancer therapy? Oncogene. 2002; 21:688–697. [PubMed: 11850797]
10. Shay JW, Bacchetti S. A survey of telomerase activity in human cancer. Eur J Cancer. 1997; 33:787–791. [PubMed: 9282118]
11. Brandes AA, Franceschi E, Tosoni A, Blatt V, Pession A, Tallini G, et al. MGMT promoter methylation status can predict the incidence and outcome of pseudoprogression after concomitant radiochemotherapy in newly diagnosed glioblastoma patients. J Clin Oncol. 2008; 26:2192–2197. [PubMed: 18445844]
12. Roldan GB, Scott JN, McIntyre JB, Dharmawardene M, de Robles PA, Magliocco AM, et al. Population-based study of pseudoprogression after chemoradiotherapy in GBM. Can J Neurol Sci. 2009; 36:617–622. [PubMed: 19831132]
13. Taal W, Brandsma D, de Bruin HG, Bromberg JE, Swaak-Kragten AT, Smitt PA, et al. Incidence of early pseudo-progression in a cohort of malignant glioma patients treated with chemoirradiation with temozolomide. Cancer. 2008; 113:405–410. [PubMed: 18484594]
14. Perry A, Schmidt RE. Cancer therapy-associated CNS neuropathology: an update and review of the literature. Acta Neuropathol. 2006; 111:197–212. [PubMed: 16463065]
15. Fizazi K, Morat L, Chauveinc L, Prapotnich D, De Crevoisier R, Escudier B, et al. High detection rate of circulating tumor cells in blood of patients with prostate cancer using telomerase activity. Ann Oncol. 2007; 18:518–521. [PubMed: 17322541]
16. Vona G, Sabile A, Louha M, Sitruk V, Romana S, Schutze K, et al. Isolation by size of epithelial tumor cells: a new method for the immunomorphological and molecular characterization of circulating-tumor cells. Am J Pathol. 2000; 156:57–63. [PubMed: 10623654]
17. Lin HK, Zheng S, Williams AJ, Balic M, Groshen S, Scher HI, et al. Portable filter-based microdevice for detection and characterization of circulating tumor cells. Clin Cancer Res. 2010; 16:5011–5018. [PubMed: 20876796]
18. Allard WJ, Matera J, Miller MC, Repollet M, Connelly MC, Rao C, et al. Tumor cells circulate in the peripheral blood of all major carcinomas but not in healthy subjects or patients with nonmalignant diseases. Clin Cancer Res. 2004; 10:6897–6904. [PubMed: 15501967]
19. Mikolajczyk SD, Millar LS, Tsinberg P, Coutts SM, Zomorrodi M, Pham T, et al. Detection of EpCAM-negative and cytokeratin-negative circulating tumor cells in peripheral blood. J Oncol. 2011; 2011:252361. [PubMed: 21577258]
20. Gradilone A, Raimondi C, Nicolazzo C, Petracca A, Gandini O, Vincenzi B, et al. Circulating tumour cells lacking cytokeratin in breast cancer: the importance of being mesenchymal. J Cell Mol Med. 2011; 15:1066–1070. [PubMed: 21352474]
21. Aktas B, Tewes M, Fehm T, Hauch S, Kimmig R, Kasimir-Bauer S. Stem cell and epithelial–mesenchymal transition markers are frequently overexpressed in circulating tumor cells of metastatic breast cancer patients. Breast Cancer Res. 2009; 11:R46. [PubMed: 19589136]
22. Mani SA, Guo W, Liao MJ, Eaton EN, Ayyanan A, Zhou AY, et al. The epithelial–mesenchymal transition generates cells with properties of stem cells. Cell. 2008; 133:704–715. [PubMed: 18485877]
23. Creighton CJ, Li X, Landis M, Dixon JM, Neumeister VM, Sjolund A, et al. Residual breast cancers after conventional therapy display mesenchymal as well as tumor-initiating features. Proc Natl Acad Sci U S A. 2009; 106:13820–13825. [PubMed: 19666588]
24. Umeoka T, Kawashima T, Kagawa S, Teraishi F, Taki M, Nishizaki M, et al. Visualization of intrathoracically disseminated solid tumors in mice with optical imaging by telomerase-specific amplification of a transferred green fluorescent protein gene. Cancer Res. 2004; 64:6259–6265. [PubMed: 15342413]
25. Soria JC, Gauthier LR, Raymond E, Granotier C, Morat L, Armand JP, et al. Molecular detection of telomerase-positive circulating epithelial cells in metastatic breast cancer patients. Clin Cancer Res. 1999; 5:971–975. [PubMed: 10353728]

26. Xu T, Lu B, Tai YC, Goldkorn A. A cancer detection platform which measures telomerase activity from live circulating tumor cells captured on a microfilter. Cancer Res. 2010; 70:6420–6426. [PubMed: 20663903]

27. Melin B, Jenkins R. Genetics in glioma: lessons learned from genome-wide association studies. Curr Opin Neurol. 2013; 6:688–692. [PubMed: 24184969]

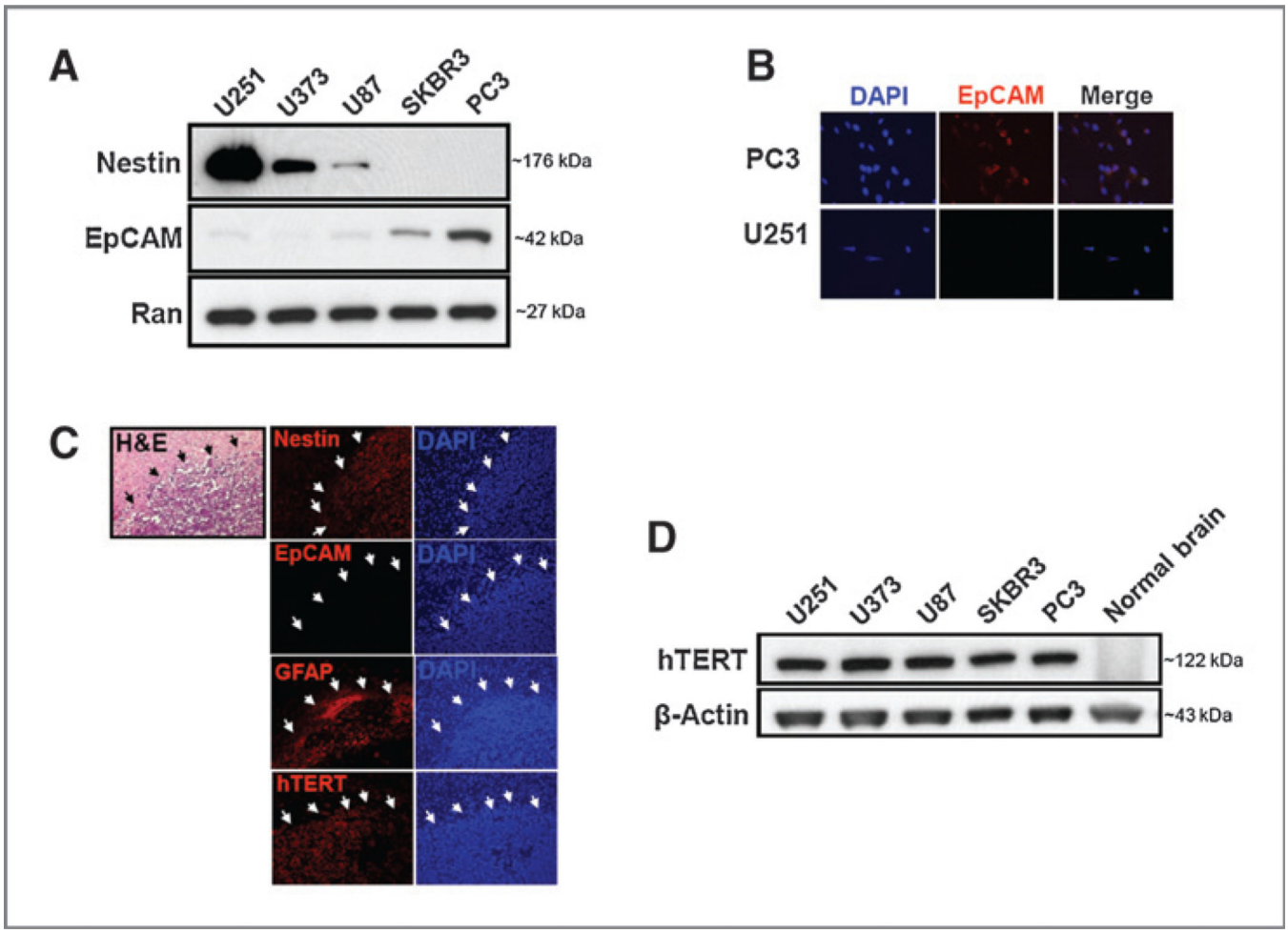

Figure 1.

Preclinical validation of telomerase-based assay for glioma tumor cell detection. A, Western blot analysis to assess Nestin and EpCAM expression was performed on human glioma cells in culture (U251, U373, and U87), alongside Nestin-negative controls: human breast cancer and human prostate cancer cell lines (SKBR3 and PC3, respectively). Nestin, EpCAM, and Ran loading control and their corresponding molecular weight markers are labeled as indicated. B, at 24 hours after probe exposure, U251 human glioma cells (bottom) were counterstained with EpCAM and DAPI as labeled, alongside EpCAM-positive control PC3 human prostate cancer cells (top) to confirm lack of EpCAM expression in glioma via immunofluorescence. Right, merge image is shown. C, U251 (constitutively expressing GFP) human glioma cells were orthotopically implanted in a nude, athymic mouse with post-mortem brain harvesting and sectioning for H&E staining and immunofluorescence staining of markers (H&E, Nestin antibody, GFAP antibody, EpCAM antibody, hTERT antibody, DAPI antibody), alongside a negative control (normal mouse brain). D, Western blot analysis was used to detect hTERT expression in human glioma cancer cells (U251, U373, and U87), human breast cancer cells (SKBR3), and human prostate cancer cell lines (PC3), alongside negative control normal mouse brain extract. hTERT and β-actin loading control and their corresponding molecular weight markers are labeled as indicated.

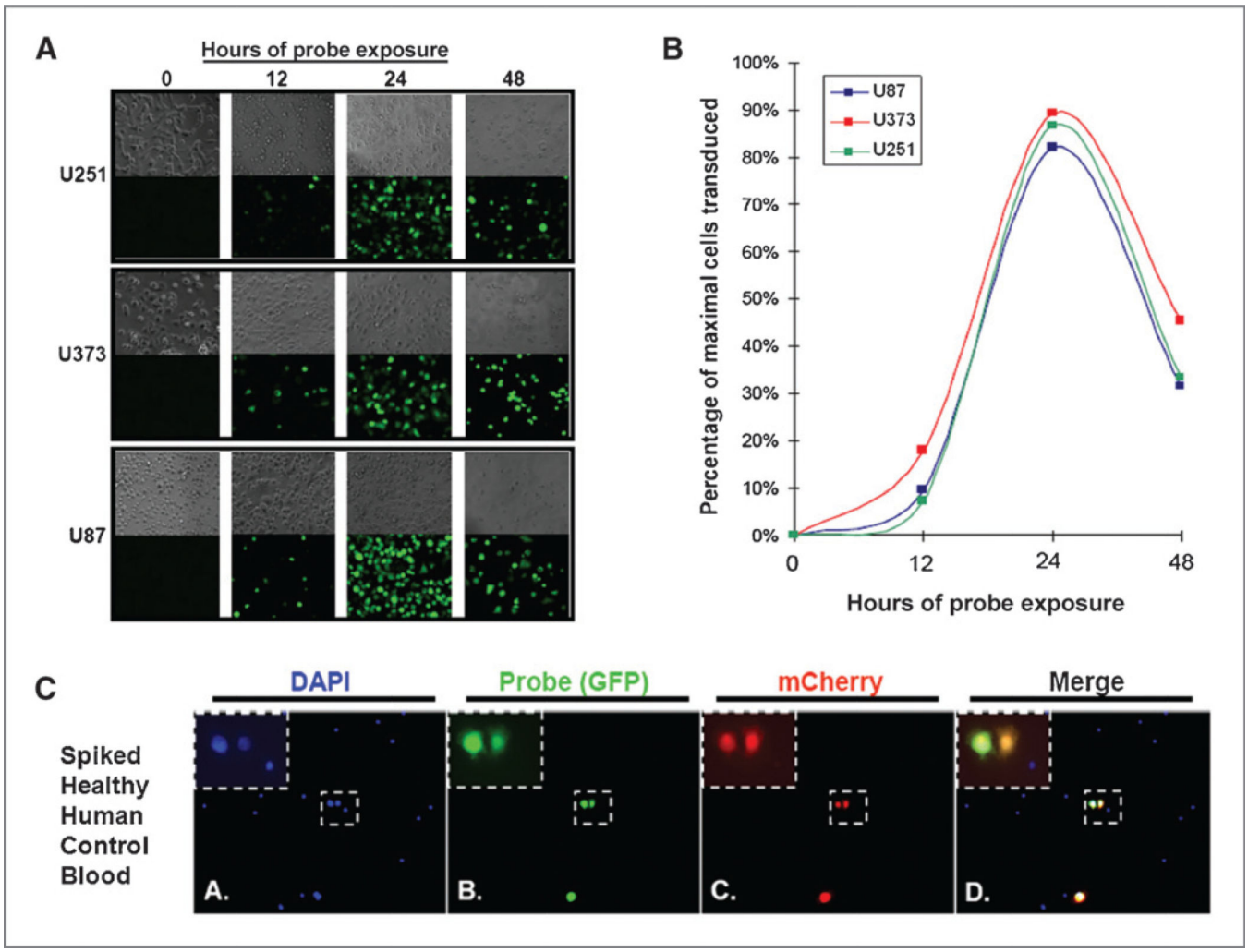

Figure 2.

Telomerase-based assay probe *in vitro* characterization for glioma tumor cell detection. A, human glioma cancer cells (U251, U373, and U87 as indicated) were infected with the probe at multiplicity of infection of 10, and (×20) images were obtained over 72 hours. Representative phase-contrast microscopy images (to depict morphology, bottom) and fluorescence microscopy images (to demonstrate GFP expression, bottom) are provided. B, at the respective indicated time points of the *in vitro* time-course experiment, automated computer software was used to determine quantity of cells transduced by the probe (demarcated by GFP expression) and total quantity of cells present on phase microscopy. Ratio of cells infected by the probe to maximal glioma cells present was calculated to establish the ideal time point for optimal specificity and sensitivity of tumor cell detection by the probe. C, U251 human glioma cells (constitutively expressing the red fluorescent mCherry protein) were spiked into control human blood followed by standard isolation and processing. Cancer cell–specific identification by the probe was demonstrated by the colocalization of mCherry (red) and GFP (green) fluorescence against a background of nontransduced WBCs (DAPI-positive, GFP-negative cells).

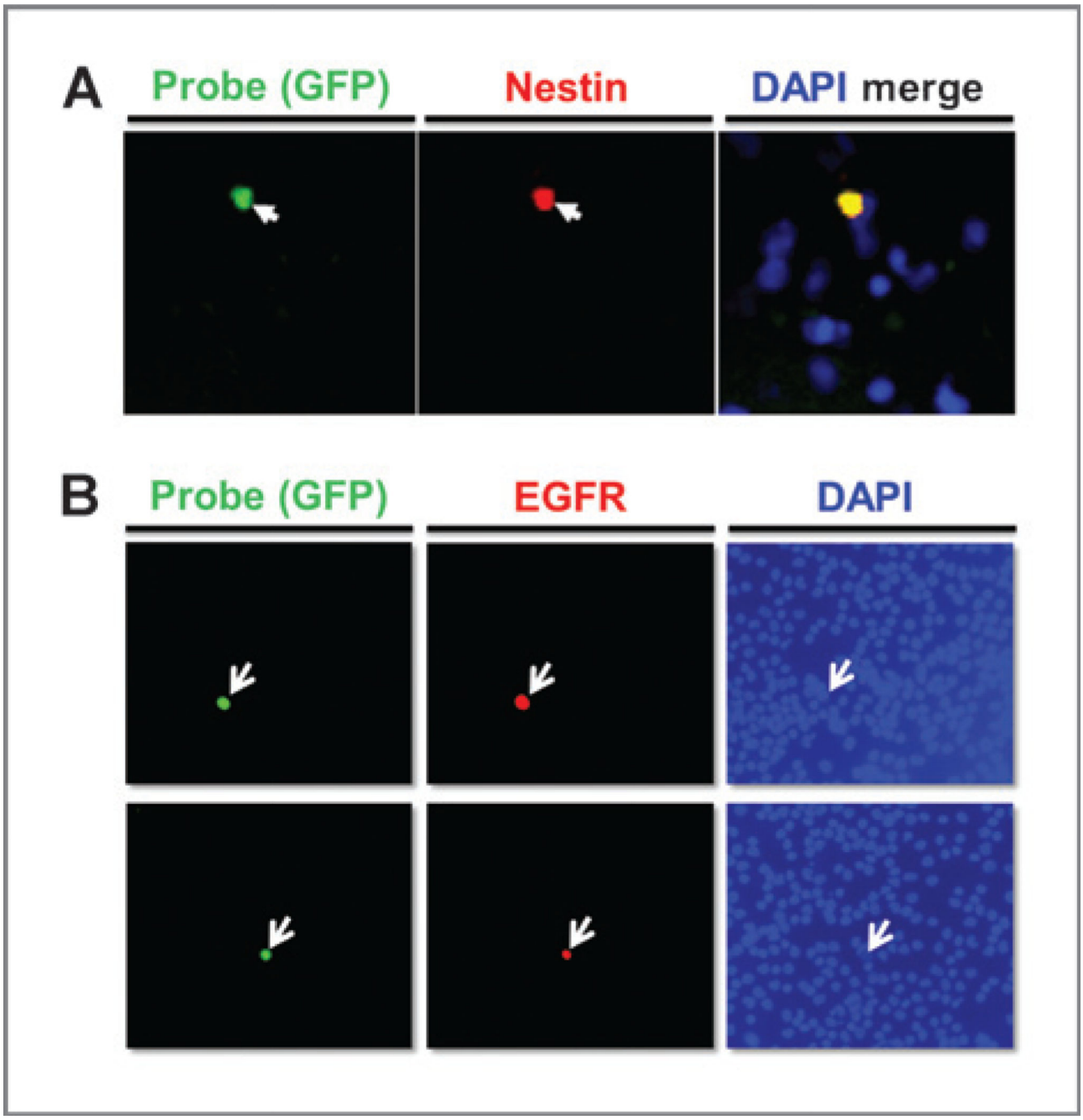

Figure 3.

Clinical results: glioma CTC detection and verification. A, a peripheral blood clinical sample was obtained from a representative patient with glioma and subjected to standard processing and enrichment for CTCs with fluorescent microscopy images acquired 24 hours following addition of the probe. Secondary immunofluorescence staining was conducted for Nestin (red). Panels show representative imaging of a CTC identified with white arrows, indicating the colocalization of a CTC after probe (green) identification and Nestin (red) staining. DAPI was used to delineate the nuclei of all cells. B, a peripheral blood clinical

sample was obtained from a patient with glioma (whose primary tumor was known to have amplification of the EGFR gene and overexpression of EGFR protein) and subjected to standard processing and enrichment for CTCs with fluorescent microscopy images acquired 24 hours following addition of probe. Secondary immunofluorescence staining was conducted for EGFR (red) as indicated. White arrows indicate the colocalization of two separate CTCs (top and bottom) identified after probe (green) identification and EGFR (red) staining. DAPI was used to identify the nuclei of cells.

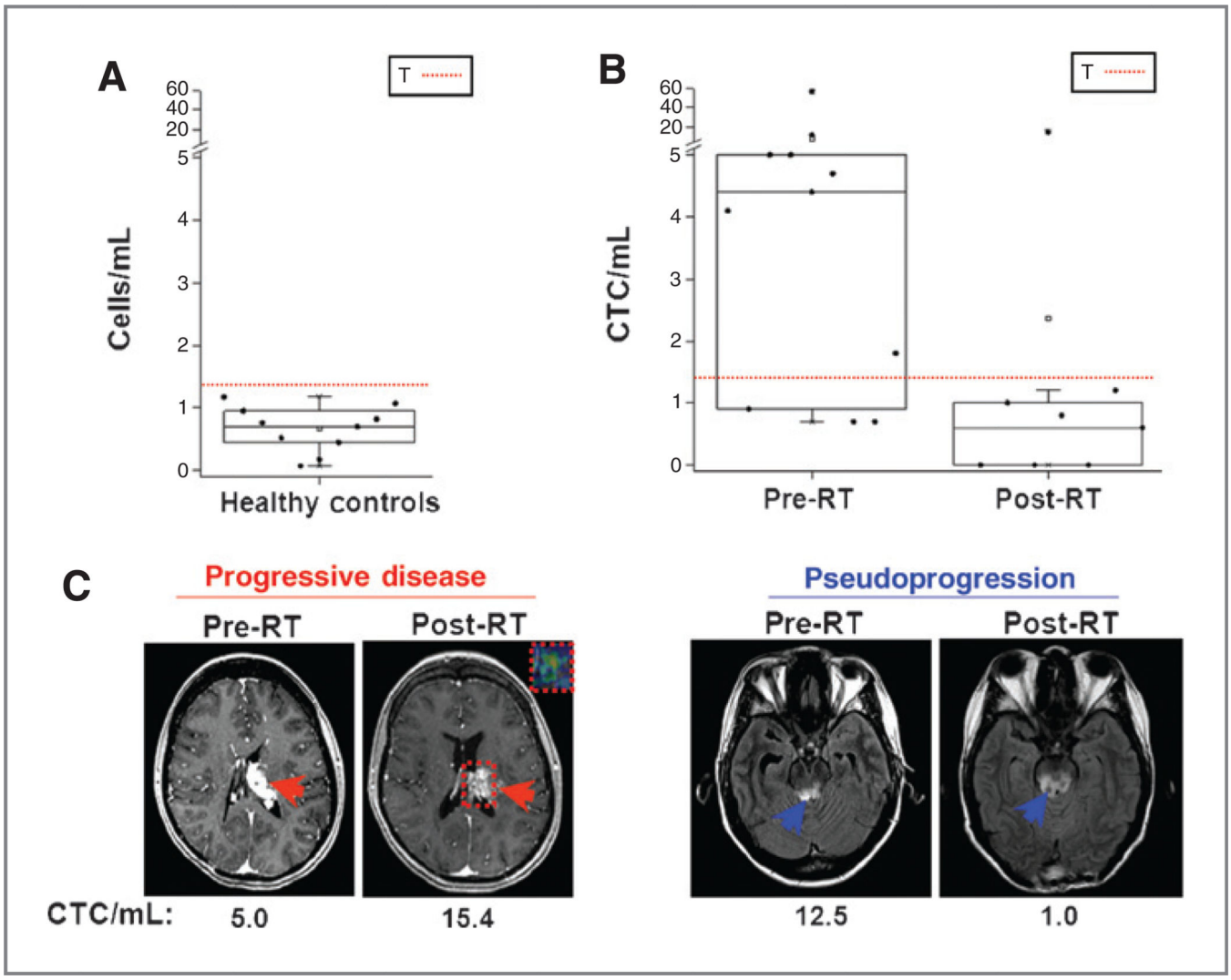

Figure 4.

Clinical results: serial enumeration to monitor treatment response in pilot study. A, peripheral blood clinical sample was obtained from preradiotherapy glioblastoma multiforme patient and subjected to standard processing and enrichment for CTCs with fluorescent microscopy images acquired following antibody (Nestin, DAPI) staining at 24 hours after exposure to the assay probe. T, classifier threshold, defined as the level observed in controls (healthy volunteers). B, CTC counts are elevated in most patients with glioma before the start of radiotherapy (Pre-RT), with marked overall decrease after treatment regimen completion (Post-RT). T, classifier threshold. C, comparison of CTC trends and brain axial MRI of "progressive disease" versus "pseudoprogression." MRI was performed within 2 weeks before initiation of radiotherapy (Pre-RT) and approximately 1 month following completion of treatment (Post-RT). CTC results (in CTC/mL) are included below axial MR images at the respective time points. Red arrows, left thalamic lesion before and following radiotherapy (left). Inset box delineated by the dotted red line (left, postradiotherapy) demonstrates the tumor area of interest and the associated advanced MRI rCBV map conducted in the postradiotherapy setting. Advanced MRI confirmed active

tumor progression after analysis of rCBV fraction. Blue arrows, MR signal abnormality in midbrain lesion and surrounding area on axial view before and following radiotherapy (right).

Table 1

Clinical characteristics of prospectively followed glioma patients

Pre-RT	Post-RT	Age	M/E	Diagnosis	WHO	Surgery	Proton/IMR	Tx (cGy)
4.4	0	87	F	GBM	IV	STR	IMRT	5,800
5.0	15.4	33	F	GBM (recurrence)	IV	Biopsy	IMRT	3,000
4.7	0.8	18	M	Anaplastic astrocytoma	III	STR	Proton	5,040, boost to 5,940
5.0	0	44	M	Anaplastic oligoastrocytoma	III	GTR	Proton	5,040
12.5	1.0	71	F	Anaplastic astrocytoma	III	STR	Proton	5,940

Abbreviations: Pre-RT, preradiotherapy; Post-RT, postradiotherapy; GBM, glioblastoma multiforme; IMRT, intensity modulated radiation therapy.